Computers & Graphics xxx (xxxx) xxx

Contents lists available at ScienceDirect

Computers & Graphics

journal homepage: www.elsevier.com/locate/cag

Special Section on STAG 2019

# Virtual reality framework for editing and exploring medial axis representations of nanometric scale neural structures

Q1 Daniya Boges[a], Marco Agus[b,*], Ronell Sicat[c], Pierre J. Magistretti[a], Markus Hadwiger[c], Corrado Calì[d]

[a] Biological and Environmental Science and Engineering Division, King Abdullah University of Science and Technology, Thuwal, 23955-6900, Saudi Arabia
[b] Visual Computing Group, Center for Advanced Studies, Research and Development in Sardinia (CRS4), Cagliari, Italy
[c] Visual Computing Center, King Abdullah University of Science and Technology, Thuwal, 23955-6900, Saudi Arabia
[d] Department of Neuroscience "Rita Levi Montalcini", Neuroscience Institute "Cavalieri Ottolenghi", University of Turin, Turin 10043, Italy

ARTICLE INFO

*Article history:*
Received 14 February 2020
Revised 21 April 2020
Accepted 12 May 2020
Available online xxx

*Keywords:*
Ultrastructural analysis
Medial axis representation
Immersive environments
Virtual reality in neuroscience

ABSTRACT

We present a novel virtual reality (VR) based framework for the exploratory analysis of nanoscale 3D reconstructions of cellular structures acquired from rodent brain samples through serial electron microscopy. The system is specifically targeted on medial axis representations (skeletons) of branched and tubular structures of cellular shapes, and it is designed for providing to domain scientists: i) effective and fast semi-automatic interfaces for *tracing* skeletons directly on surface-based representations of cells and structures, ii) fast tools for *proofreading*, i.e., correcting and editing of semi-automatically constructed skeleton representations, and iii) natural methods for interactive *exploration*, i.e., measuring, comparing, and analyzing geometric features related to cellular structures based on medial axis representations. Neuroscientists currently use the system for performing morphology studies on sparse reconstructions of glial cells and neurons extracted from a sample of the somatosensory cortex of a juvenile rat. The framework runs in a standard PC and has been tested on two different display and interaction setups: PC-tethered stereoscopic head-mounted display (HMD) with 3D controllers and tracking sensors, and a large display wall with a standard gamepad controller. We report on a user study that we carried out for analyzing user performance on different tasks using these two setups.

© 2020 The Author(s). Published by Elsevier Ltd.
This is an open access article under the CC BY-NC-ND license.
(http://creativecommons.org/licenses/by-nc-nd/4.0/)

## 1. Introduction

The brain cells, together with their processes, are complex three-dimensional structures, and improving the visual understanding of the relationships between morphological features and functional aspects of these cells is of primary importance to neuroscientists. The recent progress in digital acquisition and analysis of biological samples, e.g., brain tissues, is offering unprecedented possibilities of insights for neuroscientists. For instance, automated serial section electron microscopy (3DEM) provides electron micrographs that can reach a resolution of a nanometer per pixel, therefore revealing features ranging from full structural cellular details such as axons, dendrites, and synapses (the so called "neuropil"), to smaller intracellular organelles like synaptic vesicles. However, neuroscientists still require effective tools and applications to handle this large and complex data. Morphology data at nanoscale resolution provide domain scientists fundamental information for understanding neural processes and interaction between cellular structures [1]. Quantifications have particular relevance when extracted data are used to infer parameters allowing mathematical modelization of biological processes [2,3]. Furthermore, the challenge of making qualitative and quantitative assessments of complex and visually occluded individual cellular structures, or groups of them, is beginning to attract neuroscientists towards the use of immersive visualization paradigms. Hence, during recent years, various laboratories pioneered the use of virtual reality (VR) in supporting electron microscopy (EM) structural analysis [4–6]. However, previous pipelines were engineered around the need of exploratory analysis of brain structures for specific morphology studies [4], or neuroenergetics investigations [5,7]. More recently, the need for more efficient extraction of features of branch-based whole cell structures, either for quantification and classification

* Corresponding author.
*E-mail addresses:* magus@hbku.edu.qa, magus@crs4.it (M. Agus), corrado.cali@unito.it (C. Calì).

https://doi.org/10.1016/j.cag.2020.05.024
0097-8493/© 2020 The Author(s). Published by Elsevier Ltd. This is an open access article under the CC BY-NC-ND license.
(http://creativecommons.org/licenses/by-nc-nd/4.0/)

Please cite this article as: D. Boges, M. Agus and R. Sicat et al., Virtual reality framework for editing and exploring medial axis representations of nanometric scale neural structures, Computers & Graphics, https://doi.org/10.1016/j.cag.2020.05.024

UNCORRECTED PROOF

purposes [8], has emerged. Especially neurons, but also glia, can be adequately schematized through skeleton representations, and nowadays, various laboratories are investing important resources on creating faithful and smooth medial axis representations of brain cells. These skeleton representations can be used for various kinds of novel visual and statistical analysis. To this end, time consuming image-based manual tools [9–11] are commonly used for tracing neural processes on confocal images. More complicated automatic methods for recovering medial axis representations on nanometric scale electron microscopy stacks exist but are still in their infancy [12] and not yet routinely used for processing brain cells.

In this paper, we present a novel VR-based framework targeted on creating, proofreading, and exploration of skeleton-based representations of nanoscale brain cells surface reconstructions. The system integrates the following components:

- Fast servo-assisted semi-automatic methods for creating skeletons of complex brain cellular reconstructions.
- Tools for proof-reading (checking, correcting, comparing) medial axis representations.
- Exploration tools, e.g., for performing geometric measurements and statistical computations related to cellular structures and their skeletal representations.

The system is currently used by expert domain scientists for analysis of various cells reconstructed from the somatosensory cortex of a juvenile rat [1]. We report on a preliminary subjective evaluation of the immersive environment performed by domain experts during creation and proofreading of complex medial axis representations, as well as during analysis of organelles distributions. This paper is an extended version of the proceeding contribution presented at Smart Tools and Applications for Graphics conference [13]. We provide here a more thorough exposition, together with a more effective external semiautomatic tracing tool for editing medial axis branches. Moreover, we extended the framework to work in a monocular setup with a large scale display wall, and we carried out a user study for evaluating the performances of the system for creating and editing skeleton representations, either in the monocular display wall setup and in the stereoscopic HMD-based virtual reality setup. To our knowledge, this is the first interactive system targeted to the creation, proof-reading and analysis of skeleton-based representation of cellular structures, and the preliminary reports of usage by expert and novice users provided us promising indications that these kind of systems can positively effect the way ultrastructural analysis is carried out in neuroscience domain.

## 2. Related work

Our work deals with the application of virtual reality (VR) technologies to neuroscience investigations coupled with the computation of medial axis representations of highly detailed branched cellular brain structures. In the following, we discuss the previous work mostly related to our contribution.

*Virtual reality in neuroscience*. Due to the ubiquity of desktop systems, most commonly used visual analysis tools in neuroscience are designed as desktop applications [14,15]. However, more recently, there is general consensus that the use of stereoscopic techniques, e.g., in VR systems, can provide a more immersive way to explore brain imaging data [16], and that the increased dimensionality provided by stereoscopy is beneficial for understanding depth in the displayed scenery [17,18]. With respect to immersiveness, the effect of stereoscopy has been previously evaluated in the context of visual analysis of volume data, particularly for semitransparent volume rendering [19,20], isosurfaces [21], confocal volume images [22], and for interactive graph analysis [16,17,23]. Successful examples of applying VR technologies to neuroscience investigations include analysis of glycogen distribution related to neural morphologies [4], systems for exploring connectomes [24], systems for tracing neurons in microscope scans of primates' visual cortex [6], and the use of heat maps for representing absorption probabilities on nanoscale surface reconstructions [5]. Very recently Xu et al. [25] introduced TempoCave, a system for analyzing dynamic brain networks by exploring activity patterns in different regions in the brain, computed by processing raw data retrieved from functional magnetic resonance imaging (fMRI) scans [25]. In this work, we describe an immersive environment for performing shape analysis that is mainly targeted on skeleton representations of nanometric reconstructions. To our knowledge, it is the first application of a VR environment towards morphological analysis of medial axis representations, particularly of brain cells.

*Skeleton-based representation of surface meshes*. Medial axis representations or skeletons can be considered descriptors which jointly describe the geometry, topology, and symmetry properties of a shape in a compact and intuitive way, providing a means to capture the essence of a 3D shape [12]. Automatically or semi-automatically producing accurate skeleton representations is a challenging task. During the last decades, many techniques have been proposed, particularly by the computational geometry community, for different kinds of 3D models. For a comprehensive discussion of the recent methods for creating 3D medial axis representations, we refer the readers to state-of-the-art reports by Tagliasacchi et al. [12], and by Sobiecki et al. [26]. In general, there is a huge collection of methods to obtain 3D skeletons, which can be classified according to the input representation: mesh-based [27–30] and voxel-based representations [31]. Since our system is focused on surface representations, we will mostly consider methods that use meshes, even if our system can be considered independent from the method used for obtaining the medial axis representation of the morphology considered. The system has been designed to import skeleton representations coming from different automatic frameworks: for our initial analysis, we considered the Mean Curvature Skeleton (MCS) algorithm [27], and the Center Line Tree method [32], which are implemented in the Avizo [33] framework.

*Medial axis representations in neuroscience*. Since medial axis representations provide an adequate and convenient description for branched structures, recently, neuroscientists started exploiting them for representing complicated cellular structures, especially neurons. To this end, they derived specific metrics for comparing branched structures, i.e., trees, based on geometrical and topological features [34–36]. These metrics are then used for investigating differences and analogies between morphologies or in general for performing identification and classification [37–39]. Following this philosophy, recently Kanari et al. [40] developed a classification framework for neurons completely based on skeletons, which is based on specific topological representations, called persistence diagrams. The framework has been successfully used for objective morphological classification of neocortical pyramidal cells [8]. It has also been integrated into a more general collaborative framework for the analysis and visualization of neuronal morphology skeletons reconstructed from microscopy stacks [41]. Our proposed immersive environment addresses similar needs, and it is customized for the proofreading and analysis of skeletons of different cells, while leveraging the benefits of a VR system. We believe that 3D branched structures derived by brain cell morphologies can be more effectively analyzed by leveraging cues provided by stereoscopy and full immersion which are well suited for 3D scenes. Our framework is general and customizable, and it can be extended to integrate other geometric representations and visual encodings.

UNCORRECTED PROOF

Please cite this article as: D. Boges, M. Agus and R. Sicat et al., Virtual reality framework for editing and exploring medial axis representations of nanometric scale neural structures, Computers & Graphics, https://doi.org/10.1016/j.cag.2020.05.024

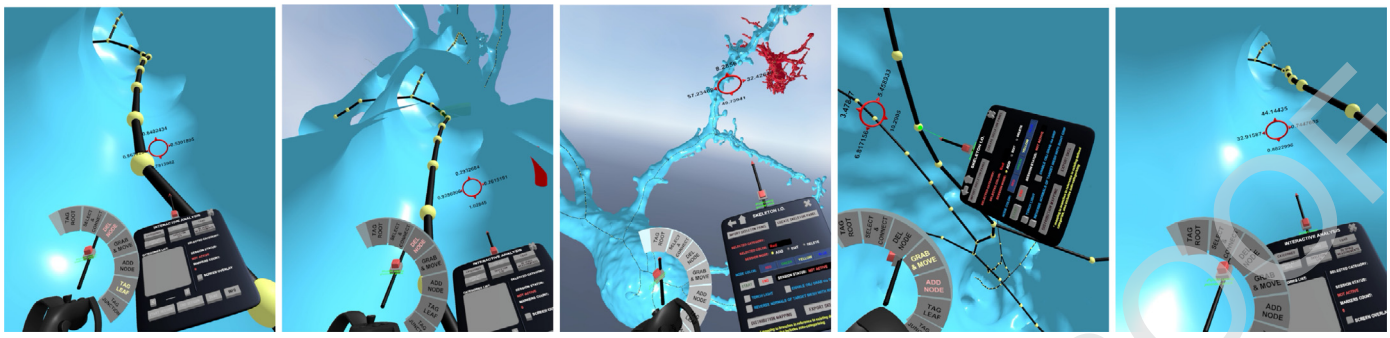

**Fig. 1.** Our proposed virtual environment enables neuroscientists to immersively create, proofread, and explore medial axis representations or skeletons of nanoscale reconstructions of brain cells. In the example scenario above, skeletons are represented as connected nodes (yellow spheres) and edges (black cylinders), while brain cells are depicted as shaded surfaces (using a light blue color in this example). (For interpretation of the references to color in this figure legend, the reader is referred to the web version of this article.)

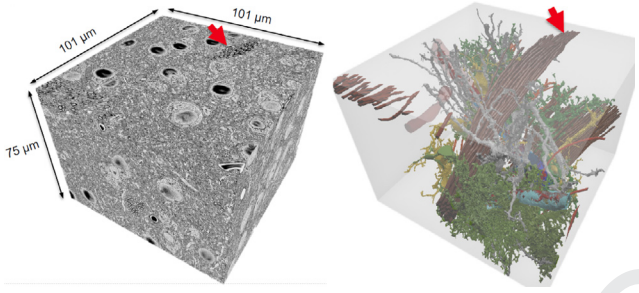


**Fig. 2. Data preparation.** Left: we tested the proposed immersive system on models reconstructed from an image stack acquired by serial electron microscopy of a sample from a juvenile rat's somatosensory cortex. Right: sparse reconstruction provides high resolution surface representation of full cellular morphologies.

## 3. Application domain: Morphology analysis in neuroscience

Before detailing the proposed immersive environment, we first provide a brief description of our particular application domain in neuroscience: the ultrastructural investigation of brain cellular morphologies at nanometric scale.

*Ultrastructural analysis*. Neuroscientists often perform ultrastructural analysis of brains samples through ex-vivo digital acquisition of very small brain portions. To this end, they use high resolution electron microscopy systems equipped with high precision cutters [42]. Through this methodology, domain scientists get 3D 8bit image stacks containing cellular membranes at nanometric resolution (see Fig. 2 left). These datasets allow them to visually individuate and annotate cellular and molecular features, such as compounds, synapses, and organelles like mitochondria. vesicles and endoplasmatic reticulum (ER). Nowadays, EM imaging technique is becoming increasingly popular in the field of connectomics, since it enables accurate reconstructions of the connections between neurons [43].

*Processing pipeline*. Given a 3D stack of images acquired by an electron microscope (Fig. 2 left), neuroscientists need to pass through different processing tasks in order to extract relevant 3D shape representations of cellular structures, in form of surface meshes (Fig. 2 right), that can be used for statistical computations, simulation, or rendering. The processing pipeline consists of carrying out dense or sparse reconstructions, by using manual, semi-automatic or automatic tools, which label the image pixels in the stack, i.e., assigning them with a unique object identifier for the various structures of interest, such as neural axons, dendrites, organelles, nuclear envelopes, etc. In this work, we used a hybrid two-step pipeline [44], composed by:

- A rough automatic segmentation performed offline through the iLastik tool [45], for finding the gross features and processes of a cell.
- A manual proofreading phase, performed through the TrackEm2 tool [46], for specifying exact object boundaries and finer details.

*Morphology features*. Once the various cells and sub-parts are labelled on a per-pixel level in the image stack, neuroscientists perform various ultrastructural analyses by studying the morphology of the following biological structures (Fig. 2 right):

- **Neurons:** composed of *axons* and *dendrites*, which are the terminals respectively sending and receiving electric signals through *boutons* and *spines*. Boutons and spines are linked and form *synapses*.
- **Glial cells:** neuroscientists mainly focus on *astrocytes*, which are metabolically involved in feeding neurons, *microglia*, which are the main form of active immune defense in the central nervous system by acting as macrophages, and *oligodendrocytes*, which produce the myelin sheath insulating neuronal axons.
- **Organelles:** domain scientists mainly focus on *mitochondria* and *endoplasmatic reticulum*, which are contained in axons, dendrites, and glial cells. They contain the machinery for chemical transformations.

Neuroscientists are interested in studying the relationships between the aforementioned structures, and perform geometric analysis for recovering parameters to be used for simulation purposes or for classification [40,47].

*Medial axis representations*. Most of the considered cells have complicated branching structures, which are very difficult to analyze using standard mesh representations (see Fig. 2 right). To this end, skeleton representations provide an effective tool for describing them and classifying the various branches, according to the size and the branching level, starting from the soma. For this reason, neuroscientists are increasingly focusing on technologies that can support them in recovering accurate skeletal representations [8,35].

## 4. System overview

The proposed system is a standard 3D framework customized to be used with a stereoscopic HMD-based setup using room scale tracking technology (VR), or with a large screen display for collaborative sessions. In VR, the system allows the user to interact with a 3D environment through two motion-tracked hand-held controllers, i.e., by pointing/selecting objects, or selecting motions through menus. When working with the display wall, a generic

Please cite this article as: D. Boges, M. Agus and R. Sicat et al., Virtual reality framework for editing and exploring medial axis representations of nanometric scale neural structures, Computers & Graphics, https://doi.org/10.1016/j.cag.2020.05.024

UNCORRECTED PROOF

**Table 1**
Notations/formats used for skeleton data.

| Algorithm/Tool | Notation/ File Format | Data Type |
|---|---|---|
| Centerline Tree (Avizo) | [ Point ID, Thickness, X Coord, Y Coord, Z Coord ]/.CSV | Points (file1) |
| | [ Segment ID, Node ID1, Node ID2, Point IDs List ] /.CSV | Branches(file2) |
| Mean Curvature Flow | [ x, y,z ] / txt | Points (file1) |
| | [ NodeID1, NodeID2 ] /.txt | Branches (file2) |
| | [ Sum of points(n), X, Y, Z, Xn,Yn,Zn ] /.txt | Points and Branches |
| Simple Neurite Tracer (Fiji) | [ NodeID, Cell Type, X, Y, Z, radius, ParentID ]/.SWC | Points with Branches |

gamepad controller can be used for input. The framework was developed on top of the Unity game engine.

*Scene representation and rendering.* The immersive environment provides real-time exploration of scenes composed of surface representations of brain cells and schematic representations of the associated medial axes or skeletons. The level of transparency of surfaces can be interactively controlled in a way to provide context for skeleton exploration. Since the system is also designed for providing endoscopic analysis of cellular processes, a torch tool is provided for shading mesh walls and dark corners during exploration. The tool is attached to one of the manipulators and can be easily used to illuminate dark areas. Basic 3D manipulation options are provided, e.g., object scaling and placement, as well as material and color assignment. Moreover, users can flip the mesh normals, in a way to have a more convenient way of examining the inner/outer mesh surfaces. With respect to skeletons, the system uses three different representations:

- **sprite-based:** 2D line segments/ribbons represent the whole skeleton geometry (implemented using Unity line renderer module);
- **Node-based:** only spheres represent skeleton nodes; depending on the skeleton data, the system can utilize only primary nodes to provide a rough representation of skeletons.
- **Complete:** skeleton nodes are represented by spheres while skeleton edges are represented by cylinders.

*Main features.* After loading the cellular morphology, the system enables users to operate on medial axis representations in two modes: *create mode* for creating skeletons from scratch, and *proofread mode* for correcting/editing previously computed skeletons. In proofread mode, the system requires that previously computed medial axes respect specific notations represented in Table 1. This notation is valid for most graph representations and is widely used by many graph processing software. Specifically, in this paper, we focused on skeletons computed through three methods:

- An automatic volume-based method [32], implemented in the Avizo framework [33] - it uses connected components for graphs, combining a union-find and a recursive algorithm.
- An automatic mesh-based method [27] - it uses iterative contraction through mean curvature flow evolution.
- A manual image-based tracer implemented in the Fiji system [10].

The system provides support for importing and exporting standard skeleton file formats that are compatible with the previously mentioned systems. It can also be easily extended to support other formats/notations.

## 5. Interactive tools

The proposed system provides interactive tools for editing/manipulating medial axis representations. We describe available interactions using 3D controllers for VR as well as for gamepad controllers for the display wall. We tried to keep most interactions similar for the two controllers in order to reduce the effort for users in terms of switching between the two if necessary. In the following, we discuss interactions based on 3D controllers but the same applies to a gamepad with the trigger button corresponding to gamepad buttons with pre-mapped functions, and 3D pointing corresponding to using the gamepad arrow and analog buttons to move the camera and the pointer. The core interactions are summarized in 7 options laid out in an arch-shaped menu (see Fig. 3 left), attached to the left 3D controller. The user can choose one of the options by first rotating his/her wrist between 0° and 180°, and then, once settled on an option, pressing the trigger buttons to select. The options provided by the system are the following:

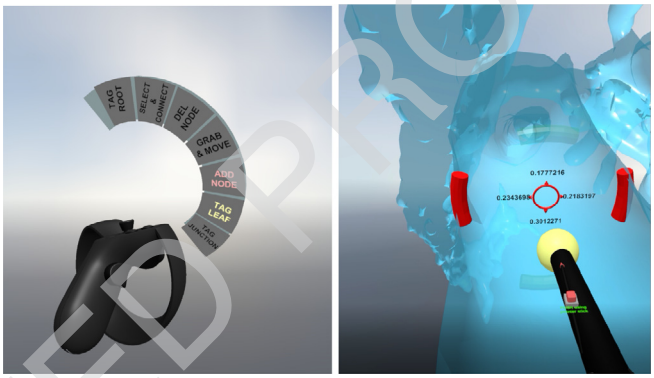


**Fig. 3. Interactive tools.** Left: an arch-shaped menu attached to the left controller allows users to select interaction mode with skeletons. Right: a stabilizer servo-assisted tool (in red) guides users through the process of skeleton branch tracing. (For interpretation of the references to color in this figure legend, the reader is referred to the web version of this article.)

- **Add Node:** using the trigger button, the user can create a node in 3D space. This process can be fully manual or controlled by a servo-assisted stabilizer. Upon creation, the system automatically pairs up nodes with each other and connects them with an edge, hence, creating a single connected path.
- **Grab and Move:** as part of the proofreading/editing process, nodes can be moved anywhere simply by grabbing them and moving them. This can be achieved thru a combination of an action grab initiated by pressing and holding of the controller's *grip* button while touching the surface of the target node.
- **Select and Connect:** using a combination of point and trigger click, the user can select two nodes subsequently and the system creates an edge connection between them (see Fig. 4 left).
- **Delete Skeleton Element:** the system allows the right controller to shoot a laser pointer by pressing on the controller touch pad. The user can then delete nodes and edges by pointing at a valid skeleton unit object followed by a trigger button click (see Fig. 4 right).
- **Tag Root, Junction, and Leaf:** a similar action of point and trigger at a specified node will save it in its corresponding skeleton file as one of these values: 0=Root, 1=Internal, 2=Leaf, 3=Junction. Tagging a node with "Leaf", "Junction", or "Root"

UNCORRECTED PROOF

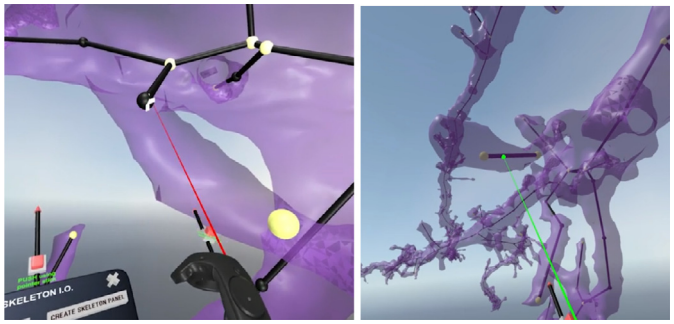

**Fig. 4. Skeleton editing.** Our system provides effective tools for rapid editing of skeleton branches. Left: adding connection between nodes. Right: removing a wrong edge from a skeleton branch.

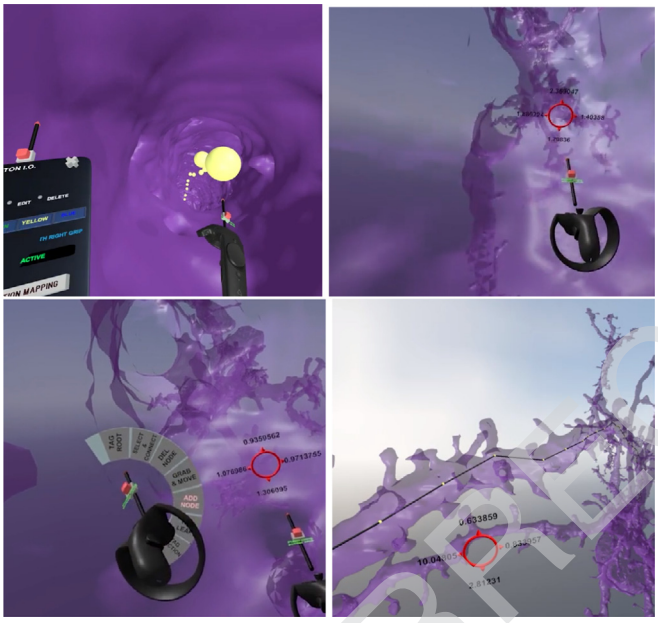

**Fig. 5. Skeleton creation.** We propose a semiautomatic and guided method for creating skeletons, based on endoscopic exploration of cell branches, and using a servo-assisted stabilizer.

marks it with a special color material and finalizes the current path as a single branch.

- **Undo:** an action that saves users the troubles of having to delete a mistake node manually, and instead, they can revert to multiple steps back during the skeleton creation process.

*Path stabilizer: tunnel metaphor.* The system provides a semiautomatic method for creating skeleton branches through one of the VR input controllers. This method is built around a visual user guide, that operates as reference when tracing the tunnel-like cellular processes through endoscopic navigation. During the exploration of the process, a path stabilizer transparently and automatically places skeleton nodes in the middle of the process section. The automatic node position computation is performed by shooting straight rays onto a number of radial directions, and computing the average distance to the surrounding wall boundaries. This simple but effective method provides a way to rapidly trace main cellular processes, and create fully controlled skeleton representations. In current implementation we use 16 rays for computing the average distance.

*Path stabilizer: tracing metaphor.* In order to speed up the tracing process of long branches exhibiting low curvature, like it happens for some neural dendrites and axons, we introduced a semiautomatic external tracing metaphor. With this tool, user is able

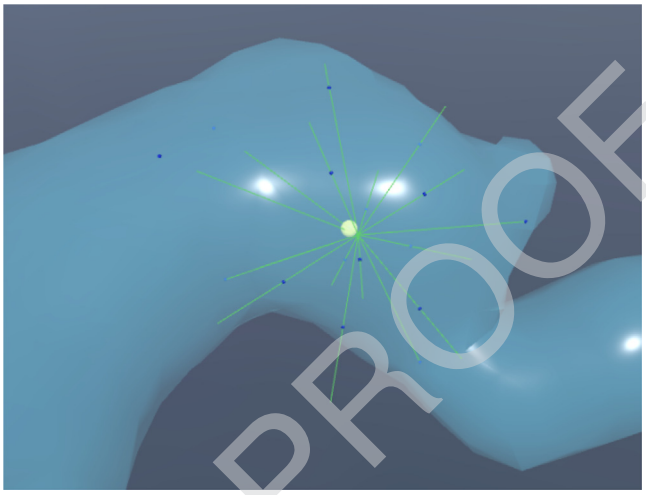

**Fig. 6. External tracing.** Users can trace branches through external 3D pointing, since a semiautomatic algorithm computes running barycenters through multiple iterative ray casting.

to follow the path of the specific through 3D pointing, while the system uses ray casting for intersecting the branch, and, starting from the ray, an iterative approach shoots different rays similarly to the previously described tunnel metaphor. In order to accelerate the computation of nearest neighbors, we use a KD-tree data structure. The running barycenters of the different ray intersections are added as nodes in the current skeleton branch. Even in this case, in current implementation we use 16 rays for computing the running barycenter. This method proved to be very fast and effective for processes not exhibiting sharp features and bumps (see Section 7). Fig. 6 shows an example of the algorithm for computing a node.

## 6. Setup and dataset

Our proposed immersive system is used by neuroscientists for performing real-time creation, proofreading/editing, and exploration of brain cell reconstructions based on medial axis representations.

*Implementation details.* The immersive system has been developed and deployed using the Unity game engine (version 5.6.3, via C# scripting). For VR, it uses SteamVR and the VRTK software packages [48], which provide smooth immersive system-user interaction as well as cross-hardware setup compatibility. In this way, the same application can be used on various VR setups, like Oculus Rift [49] or HTC Vive [50]. For computing automatic skeletons, and for other preprocessing tasks, we implemented and used C++ applications and Python scripts. In addition, we used Avizo (a commercially available data analysis/visualization software framework) for computing high-quality skeletons, and preprocessing was carried out on a workstation equipped with two CPUs of 10 cores each (see Table 2 for additional details).

*Data preparation.* For testing purposes, we considered five complex cellular structures reconstructed from a p14 rat somatosensory cortex. We selected different kinds of cells to show different levels of complexity: two neurons, two microglia, and one astrocyte [1]. The cells were reconstructed from a high-resolution EM stack with approximated size of $100\mu m$ X $100\mu m$ X $76.4\mu m$ (see Fig. 2 left). The reconstruction process was performed through a semiautomatic process [44] involving customized components and public domain software like iLastik [45] and TrakEM2 [46]. The output of the reconstruction process is a series of high resolution triangular meshes representing the cellular morphologies (see Fig. 2 right). Furthermore, each cell was optimized in a way to be

UNCORRECTED PROOF

Please cite this article as: D. Boges, M. Agus and R. Sicat et al., Virtual reality framework for editing and exploring medial axis representations of nanometric scale neural structures, Computers & Graphics, https://doi.org/10.1016/j.cag.2020.05.024

**Table 2**
Machines used for immersive environment and data preparation.

| Machine | OS | Task | Specs |
|---|---|---|---|
| Asus ROG G703G | Windows 10 Pro- | Immersive environment | 32GB DDR4, Intel Core i9-8950HK 4.8 GHz, Nvidia GTX 1080 8GB GDDR5X, 2X 256GB PCIE SSD + 2TB SSHD FireCuda. |
| Supermicro | Linux CentOS 7 | Data processing and skeleton creation | 1TB memory, Intel(R) Xeon(R) Gold 6150 CPU2.70GHz (18 Cores), Nvidia GK104GL Quadro K5000, N/A |

watertight and without non-manifold edges and vertices, and in a way to preserve all important morphological features. To this end, we used public domain mesh processing tools like Blender [51], Meshlab [52], and Ultralizer, a geometry processing tool contained inside the suite NeuroMorphoVis [41]. For getting automatic medial axis representations of the considered morphologies, we used the Mean Curvature Skeleton algorithm [27], as well as the Centerline Tree module both available in Avizo [32]. In Table 3 we report on the cell morphologies and the associated skeleton representations. Specifically we provide visual representations of the morphologies, together with information about their shapes and sizes in terms of vertex counts, visual representations of automatic skeletons, and skeleton graph statistics (number of nodes, number of edges, and number of branches).

*Hardware setups*. We tested the VR application on a gaming laptop equipped with an Nvidia GTX 1080 8GB GDDR5X GPU. We used the laptop to drive two different display setups (see Fig. 8):

- A stereoscopic immersive Head Mounted Display (HMD) Oculus Rift S [53] with sensors embedded in a way to lower the bulkiness of the system and increase portability. The display uses a single fast-switch LCD panel with a resolution of $2560 \times 1440$ with a refresh rate of 80 Hz, field of view of 110 degrees on a workspace of $3.5\,\text{m} \times 3.5\,\text{m}$;
- A monocular collaborative large-scale display wall composed of an array of tiled $3 \times 4$ Narrow Bezel Monitors (55") ($7680 \times 3240$ pixels) for a total resolution of around 25 Mpixels. For the monoscopic display setup, the Oculus Rift input devices were substituted by an Xbox gamepad controller.

The two different setups provide different working environment in which the tools can be used as direct pointers for performing editing operations on the scene. The proposed interacting metaphors are general and can be adapted to different setups, using different kind of controlling devices, like touch devices or gestures [54]. According to the taxonomy presented by Mendes et al. [54], the considered setups are the following: an immersive one, with 3D controllers physically providing a direct metric control over the scene represented in a virtual workspace, and a gaming one, with gamepad controllers controlling a 2D display wall, in an indirect way. Regarding the design choices, we decided to do not use the same controllers in both setups since the oculus controllers are natively connected to a real 3D physical setup, and we believe they would not be naturally understood if coupled to a monoscopic display setup.

## 7. Results

We carried out a preliminary assessment of the system to understand how is the usability in the context of exploratory analysis of different kind of cells. We report here on two kind of evaluations: a subjective qualitative assessment performed by expert users on complete creation of skeleton representations of entire cells, and an user study for evaluating the performance of the system for editing tasks either in HMD-based stereoscopic setup and Wall-based monoscopic setup. Finally we report on a use case for measurement analysis on distributions of branched-like organelles.

### 7.1. Expert evaluation

A preliminary evaluation of the system was performed by two expert neuroscientists on cells of Table 3. Domain scientists were particularly interested in obtaining accurate and clear skeletal representations to be used as descriptors of highly intricate cellular structures. In general, they want to have precise control of medial axis representations, in a way to be able to clearly separate main processes from fine details that have different biological meaning (for example dendritic shafts and spines in neurons). In this sense, most automatic systems provide "dirty" medial axis representations, thus we expected that an interactive tool helping in cleaning skeletons would receive a positive feedback. Moreover, we expected that the immersiveness provided by virtual reality could improve the creation and editing process.

*Skeleton creation from scratch*. Neuroscientists used the system for creating skeletons from scratch on two neural morphologies. In Table 4, we show statistics about the skeleton creation process, with different tracing metaphors (internal and external) and different display setups (VR-based and Wall-based). The procedure consisted of exploring the surface models in order to select the main processes, and trace the branches from inside the cells, i.e., similar to an endoscopic navigation/view. Domain scientists felt comfortable in recognizing main processes, e.g., dendrites and spines, in a way to correctly trace the medial axis of interest. Moreover, they felt quite comfortable with the path stabilizer, which reduced the number of input actions on controllers. A comparison of creation times between the two different display setups and the different tracing interfaces shows that expert users were faster when using external tracing metaphor with stereoscopic VR setup (almost 2X with respect to the worst case according timings in Table 4).

*Skeleton proofreading/editing*. Automatically computed skeletons were examined by domain scientists through the proposed system (see Fig. 7). They used the system for comparing skeletons automatically computed through Mean Curvature Flow (MCS [27]), and Centerline Tree (CLT [32]). They concluded that both the methods considered were able to cover all the morphology features of interest. However, skeletons produced by CLT appeared to be too highly detailed, with a number of wrongly assigned branches as well as disconnected parts. Table 5 shows the difference in the total number of branches, nodes and edges for each algorithm for all five cells. In general, domain scientists found that skeletons produced by MCS algorithm contained a lower number of artifacts. For this reason, in all considered cases, they preferred to perform editing and cleaning on skeletons computed through MCS algorithm. To this end, they carried out a series of checks depending on the type of cell, and on the biological significance of the various features:

- Identify main branches by tagging their nodes as either leaf, end of branch, or internal nodes. The system identifies all node types based on the degree of each one in the graph tree. However, some needs to be adjusted based on the cell's biological features. Using the VR interactive menu, the user points at a node with the VR controller's laser pointer and then clicks on the trigger button to tag it. The node's color material will switch color indicating that it is saved in the system based on the tagging feature. In the case of neurons, the main branches would be all dendrites, excluding any other features e.g., spines.

UNCORRECTED PROOF

Please cite this article as: D. Boges, M. Agus and R. Sicat et al., Virtual reality framework for editing and exploring medial axis representations of nanometric scale neural structures, Computers & Graphics, https://doi.org/10.1016/j.cag.2020.05.024

**Table 3**
**Morphologies and Mean Curvature Skeletons (MCS) of 5 biological cells.** Cells are computed automatically through [27] and proofread and cleaned through our Virtual Reality system. Together with pictorial representations, we report on cell sizes, total times for proofreading and cleaning, and skeleton statistics.

| Name | Picture | Vertices | Time | Before cleaning | Nodes-Edges-Branch | After cleaning | Nodes-Edges-Branch |
|---|---|---|---|---|---|---|---|
| Neuron1 | 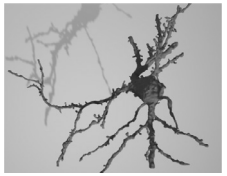 | 49,628 | 10.00 |  | 1569\| 1573\| 201 |  | 1318\| 1321\| 25 |
| Neuron2 | 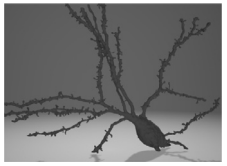 | 78,215 | 15.28 |  | 1,619\| 1,629\| 357 |  | 1215\| 1223\| 20 |
| Microglia1 |  | 48,015 | 09.00 |  | 1,463\| 1,479\| 165 |  | 1443\| 1456\| 62 |
| Microglia2 | 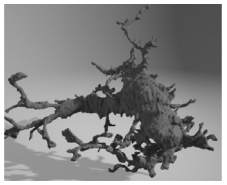 | 125,532 | 13.53 |  | 2,105\| 2,122\| 260 |  | 2060\| 2077\| 111 |
| Astrocyte | 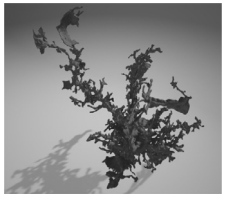 | 211,004 | 25.16 |  | 4,055\| 4,137\| 854 |  | 3906\| 3983\| 296 |

UNCORRECTED PROOF

Please cite this article as: D. Boges, M. Agus and R. Sicat et al., Virtual reality framework for editing and exploring medial axis representations of nanometric scale neural structures, Computers & Graphics, https://doi.org/10.1016/j.cag.2020.05.024

**Table 4**
Statistics on skeletons generated semi-automatically from scratch for Neuron1 and Neuron2 morphologies.

| Cell Name | Skeleton | Time Stereo Int | Time Stereo Ext | Time Mono Int | Time Mono Ext | Nodes\| Edges\| Branches |
|---|---|---|---|---|---|---|
| Neuron1 |  | 25:13 | 14:24 | 29:55 | 25:28 | 481\| 480\| 25 |
| Neuron2 |  | 30.50 | 14:35 | 22:54 | 24:11 | 629\| 628\| 20 |

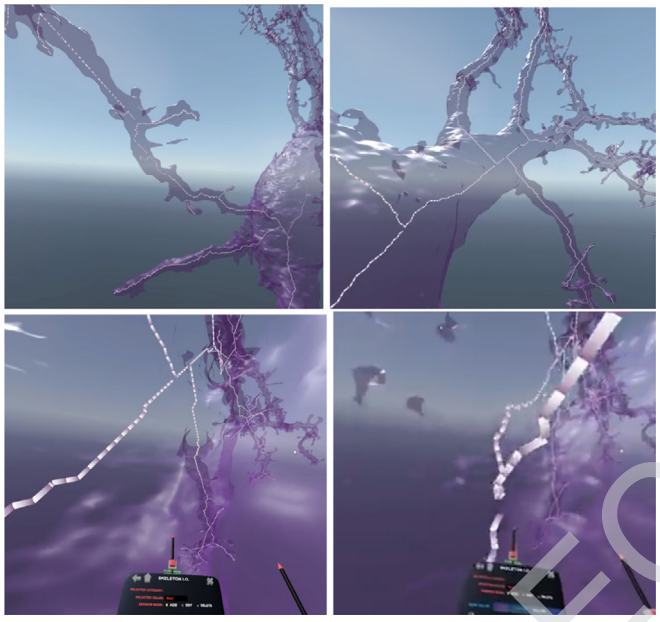

**Fig. 7. Skeleton proofreading.** Our system enables domain scientists to perform effective proofreading of skeletons by using endoscopic and external metaphors.

**Table 5**
Neuron1 and Neuron2 skeleton properties as generated via Mean Curvature Skeleton (MCS) and Centerline Tree (CLT) algorithms.

| Cell Name | Algorithm | Nodes\|Edges\|Branches |
|---|---|---|
| Neuron1 | MCS | 1569 \| 1573 \| 201 |
| | CLT | 7719 \| 7328 \| 361 |
| Neuron2 | MCS | 1619 \| 1629 \| 357 |
| | CLT | 9655 \| 9530 \| 516 |

- In the case of highly-detailed skeletons, one would encounter duplicate nodes and edges, disconnected parts, loops, and out of track skeletonization. Neuroscientists tried to delete all defects through an iterative manual process.
- The soma area should be clear from any branching so neuroscientists "cleaned" these parts by deleting all branches and merging them into one.

In last two columns of Table 3, we show the proofreading outputs for all the considered cells. In general, domain scientists found the proofreading task comfortable and accurate, and they particularly appreciated the immersiveness of the system for checking features and recognizing defects. For comparison, we asked expert neuroscientists to perform skeleton cleaning by using the external tracing metaphor together with the wall display setup: timings recorded for Neuron1 (27 m58 s) and for Neuron2 (46 m10 s) provided us evidence that the monoscopic setup associated to the external interface is not comfortable for cleaning skeletons.

*Discussion.* In general, one of the drawbacks of dealing with an immersive environment on long sessions (20 min and more), is the symptoms of cybersickness and fatigue. This happened also for our system, and, during the sessions, users needed to take breaks every 15 min when performing each task. To this end, the system allows for multiple saves across sessions, and the user can retrieve the file anytime and continue where he/she last stopped. From this point of view, users liked the display wall setup in case of cyberfatigue, since they could sit, and rest while still working on the task. As general impression, the system was considered very useful for both proofreading/cleaning pre-exported skeletons, as well as for creating skeletons from scratch. In particular, neuroscientists trained in neurite tracing found very effective how the tool automatically provides a centerline, without the hassle of having to place it manually. Although the process of creating skeletons from scratch in VR can be time-consuming, automatic tools can make a lot of mistakes, and the time saved on the manual tracing would be lost on the proofreading anyways. This largely balanced the costs/benefits of the two approaches. Several factors contributed to make the creation process time consuming, mainly technical. One factor involves the order of tracing the various branches. Specifically, in some cases, users started tracing from the soma and proceeded towards the tips, while in other cases they made the opposite choice, by starting from the tip of the most extended branch and tracing towards the soma. We also experienced that another

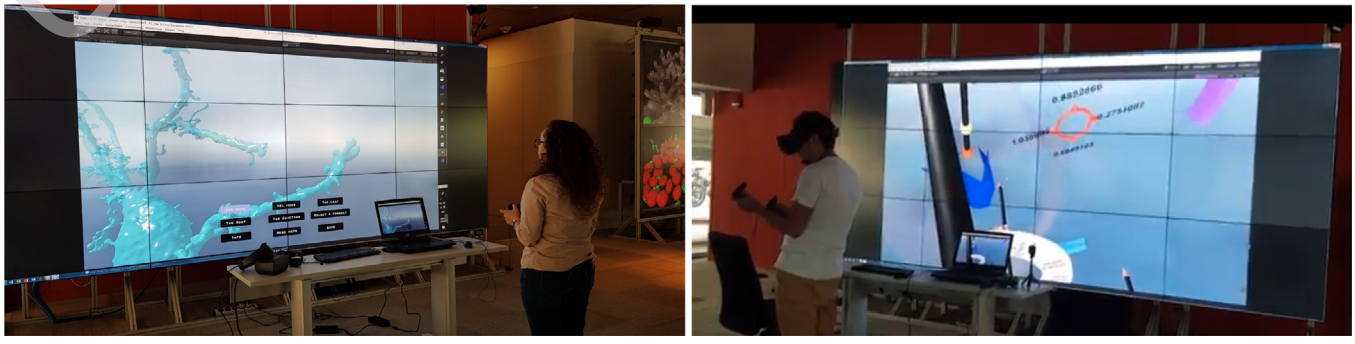

**Fig. 8. Display setup for user study.** We evaluated the system performance under different display conditions: large scale monoscopic display (left), and head mounted stereoscopic display (right).

Please cite this article as: D. Boges, M. Agus and R. Sicat et al., Virtual reality framework for editing and exploring medial axis representations of nanometric scale neural structures, Computers & Graphics, https://doi.org/10.1016/j.cag.2020.05.024

UNCORRECTED PROOF

source of error was the path-stabilizer, in cases where the user happened to release a node at a bifurcation spot. Since the path-stabilizer is based on the concept of ray-casting, users needed to take care of correctly keeping the VR controller within the walls of the cellular structure. Issues with the stabilizer were experienced also in cases when the cell's main branch has too many spines within close distance to each other. In such situations, neuroscientists sometimes preferred to disable the stabilizer and operate on a full-manual mode. In general, we noticed that most creation issues were alleviated as users gained experience with the system, and we think that performance should dramatically improve once users repeat the process for many cells, i.e., after further training and experience. From the quality point of view, neuroscientists were satisfied with skeletons generated from scratch in VR, since they appeared well-structured and represented precisely the biological structure of the cells, tailored accordingly to their experience and knowledge about cell morphology. Regarding the proofreading task, domain scientists performed very well in checking and editing all five skeletons. They experienced some problems only with the Astrocyte, which took around 25 minutes to be proofread and edited. This is due to the fact that astrocytes have very complicated branched structures (see Table 3), where main processes are very difficult to recognize at first sight even for expert domain scientists.

### 7.2. User study

The use of Virtual Reality in Neuroscience is still at its early stages [5,55], therefore the user studies for evaluating the performance of Virtual Environments for editing tasks are currently designed almost from scratch, because of the lack of standardized guidelines [56]. In our case, we aimed to assess the performance of the system for creating and modifying skeleton representations of brain cells. To this end, we involved 12 users with different level of experience, and we asked them to perform specific tasks under different conditions. We measured times and accuracy, and we assessed the fatigue and comfort through NASA-TLX questionnaire [57]. In the following we detail the design of the user study and the outcomes of evaluation. The main goal of the study was to evaluate the effects of HMD and wall display on system performance, and whether users felt more comfortable with external or internal tracing metaphor for editing purposes (see Fig. 8). The study took place in the visualization lab facility of King Abdullah University of Science and Technology, and in the department of Anatomy at University of Turin.

*Design and protocol.* Subjects were asked to perform various partial tasks on the system, using HMD or Wall display, and using internal or external metaphor for editing operations. Specifically, after a period for training and getting comfortable with the various setups and tools, we asked users to edit the skeleton of a brain cell in the following way:

- Trace a full branch.
- Correct a branch by removing nodes and links.

The branches to be traced were chosen randomly from two long dendritic processes of Neuron1 and Neuron2 (see Fig. 10). Before each task, the user was shown how the task is performed and how the joystick controls are being operated. They were given a few minutes to practice the task until they were comfortable enough to go ahead and start their mission. Water and refreshments were offered at all times during the study. Equipment were wiped and cleaned thoroughly with antibacterial wipes after each use.

The two tasks were repeated randomly under different conditions, depending on the display type and the tracing metaphor for a total of 8 tasks (see Fig. 9). Between each task a break of five minutes was given to subjects. After one task was complete (under the 4 conditions), users were asked to fill a 6 questions NASA-TLX form for comparing mental demand, physical demand, temporal demand, performance, effort and frustration (see Table 6), with a 5 value Likert scale score ranging from low to high [57]. During the tasks we measured the total time for performing the tasks, and the paths of the traced branch. The tests were designed in a way that users did not need more than 60 min for training, completing all tasks, and filling the forms. Think-out-loud comments were also recorded during sessions.

*Quantitative performance.* For measuring performance in creation and editing tasks we compared branches obtained by users with respect to ground truth obtained by MCS [27]. Fig. 11 shows an example of a branch created by a user (in pink), and the corresponding ground truth (in blue). Fig. 12 shows performance results for the tests related to accuracy for trace branches and the completion time, obtained after filtering very few outliers of subjects exhibiting really poor performance. We show results in form of boxplots: the bottom and top of each box are the first and

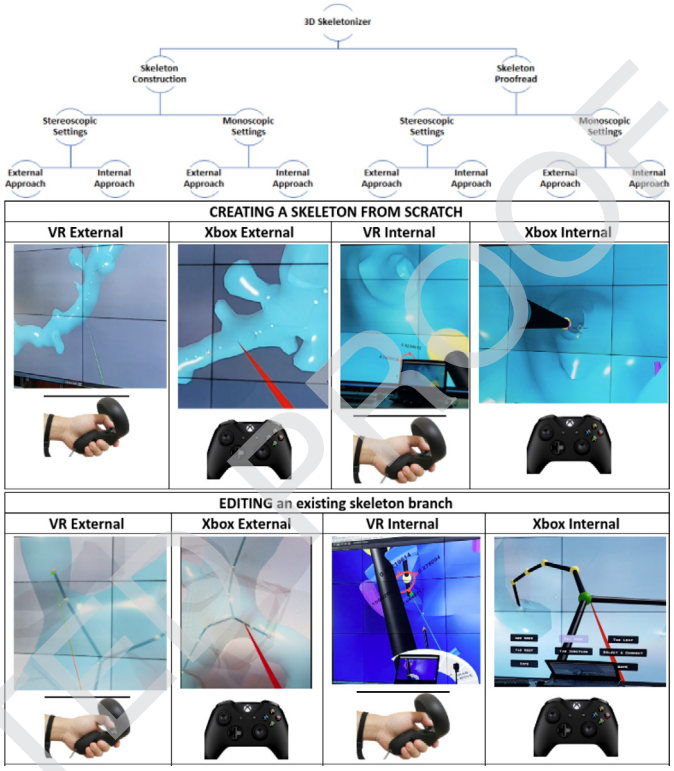


**Fig. 9. User study protocol:** subjects were asked to perform eight skeleton editing tasks under different conditions related to tracing metaphor and display setups.

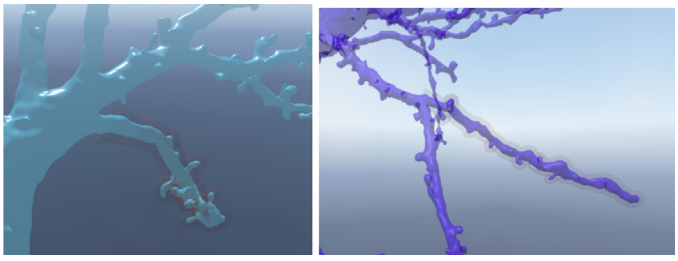

**Fig. 10. User study data:** subjects were asked to perform eight editing tasks under different conditions on two long processes from Neuron1 (left) and Neuron2 (right).

UNCORRECTED PROOF

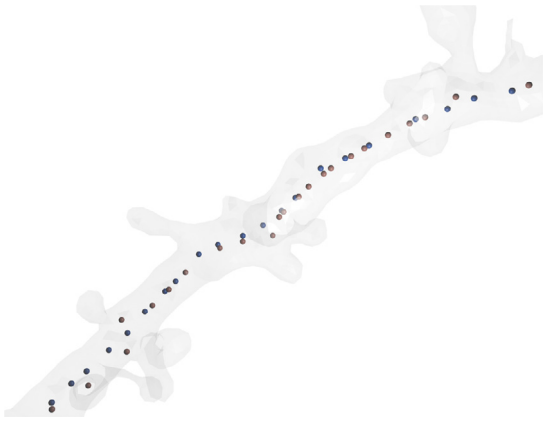

**Fig. 11. Accuracy measurement.** We measure the accuracy of branch creation through Hausdorff distance between the ground truth branch computed by MCS [27] (in blue in this example), and the branch traced by subjects (in pink in this example). (For interpretation of the references to color in this figure legend, the reader is referred to the web version of this article.)

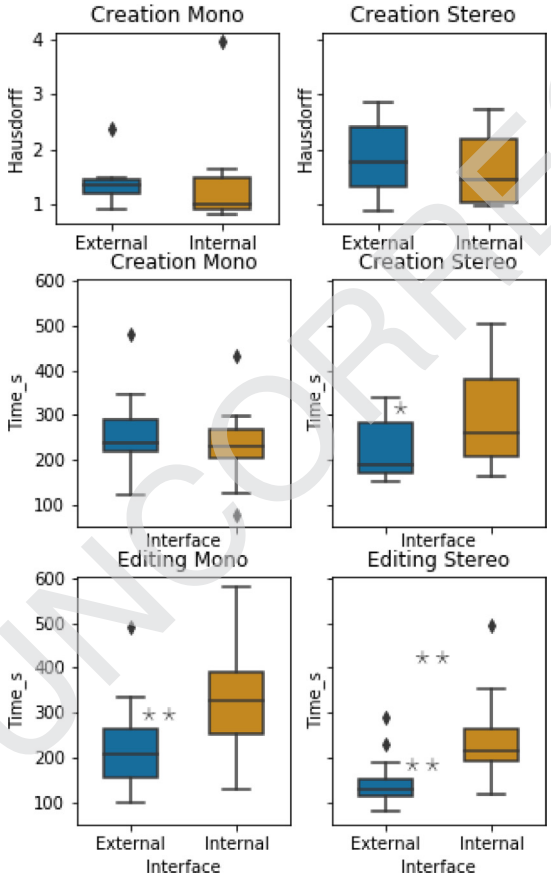


**Fig. 12. Quantitative performance.** Boxplots of accuracy performance for creation task (Hausdorff distance with respect to ground truth computed with Mean Curvature Flow in top row), and time performance for creation task (middle row) and editing task (bottom row). The bottom and top of each box are the first and third quartiles, the black line inside the box is the second quartile (the median), and the ends of the whiskers extending vertically from the boxes represent the lowest datum still within 1.5 IQR (inter-quartile range) of the lower quartile, and the highest datum still within 1.5 IQR of the upper quartile.

third quartiles, the black line inside the box is the second quartile (the median), and the ends of the whiskers extending vertically from the boxes represent the lowest datum still within 1.5 IQR (inter-quartile range) of the lower quartile, and the highest datum still within 1.5 IQR of the upper quartile. Outliers are indicated as small circles. On top we show the accuracy of tracing in form of Hausdorff distance in $\mu m$ between the branch created by subjects and the ground-truth branch computed through Mean Curvature Flow [27]: given two point sets $\mathbf{X}$, $\mathbf{Y}$ representing two branches, we measure the symmetric Hausdorff distance [58] as the maximum of the asymmetric directed Hausdorff distance $H(\mathbf{X},\mathbf{Y}) = \max(\hat{H}(\mathbf{X},\mathbf{Y}),\hat{H}(\mathbf{X},\mathbf{Y}))$, where the directed Hausdorff distance is defined as

$$\hat{H}(\mathbf{X},\mathbf{Y}) = \max_{x\in\mathbf{X}}(\min_{y\in\mathbf{Y}}\|x-y\|). \quad (1)$$

ANOVA on the Hausdorff distance showed no effects due to the display for accuracy ($1.49 \pm 0.88$ with Mono setup versus $1.74 \pm 0.72$ with Stereo setup). Also the different interfaces do not appear to affect accuracy ($1.63 \pm 0.65$ with External interface versus $1.60 \pm 0.96$ with the Internal interface). On the bottom we compare the task completion time, either for the creation process (middle row) and the editing process (bottom row). ANOVA revealed an effect on interface when used with Stereo setup ($p = .06$ with $F = 3.893314$) for the creation task, with $T = 218 \pm 64.6$s for external interface, and $T = 292 \pm 117.7$ s for internal interface, indicating that the external interface appears to be faster for creation especially in VR setup. Moreover, ANOVA revealed an important effect for editing either related to the display setup ($p = .007$ with $F = 8.106935$) and the interface ($p = .001$ for $F = 12.24$), indicating that external interface is perceived more comfortable and users perform editing tasks faster when they use the VR setup.

*Qualitative performance.* Table 6 shows the questions and results of NASA-TLX questionnaire proposed to subjects after tasks in order to evaluate their perception of performance, satisfaction, fatigue and stress under the different conditions.

Fig. 13 shows the boxplots of answers on a Likert scale (1=low,5=high). ANOVA on answers revealed a slight effect for self satisfaction during the tracing task due to display setup ($p = .03$ and $F = 5.29$ for question Q4 in favor of VR setup), and effects on stress of display ($p = .1$ and $F = 2.81$ for question Q6 in favor of VR setup), and interface ($F = 3.93$ and $p = .05$ for question Q6 in favor of external tracing). With respect to the editing task, ANOVA revealed significant effects related to the display for mental demand ($F = 12.67$ and $p = .001$ for question Q1 in favor of VR setup), physical demand ($F = 12.86$ and $p = .0008$ for question Q2 in favor of VR setup), fatigue ($F = 8.14$ and $p = .006$ for question Q5 in favor of VR setup), and stress ($f = 3.32$ and $p = .07$ for question Q6 in favor of VR setup). No significant effects were found due to the different editing interface.

*Discussion.* By observing the behavior of users with the system, we could note that the learning curve was rapid and the process per-se was pretty straight forward. In general, while performing the tasks, all operations required some time for the user to learn how to switch from one function to another one. To note also in this case the learning curve was pretty fast for experienced tracers. For the usage of the system on display wall setup, we realized that it is a factor of advantage if the user is a gamer, when using the XBOX controller: expert gamers appeared to be more comfortable and to navigate blindly and effortlessly. In general the user study revealed that subjects feel more in control when in VR, since the orientation, navigation and interaction is more natural, and they can contribute with body, head and hands and not just two joysticks that restrict movement, eyesight and perspective. Since we

UNCORRECTED PROOF

Please cite this article as: D. Boges, M. Agus and R. Sicat et al., Virtual reality framework for editing and exploring medial axis representations of nanometric scale neural structures, Computers & Graphics, https://doi.org/10.1016/j.cag.2020.05.024

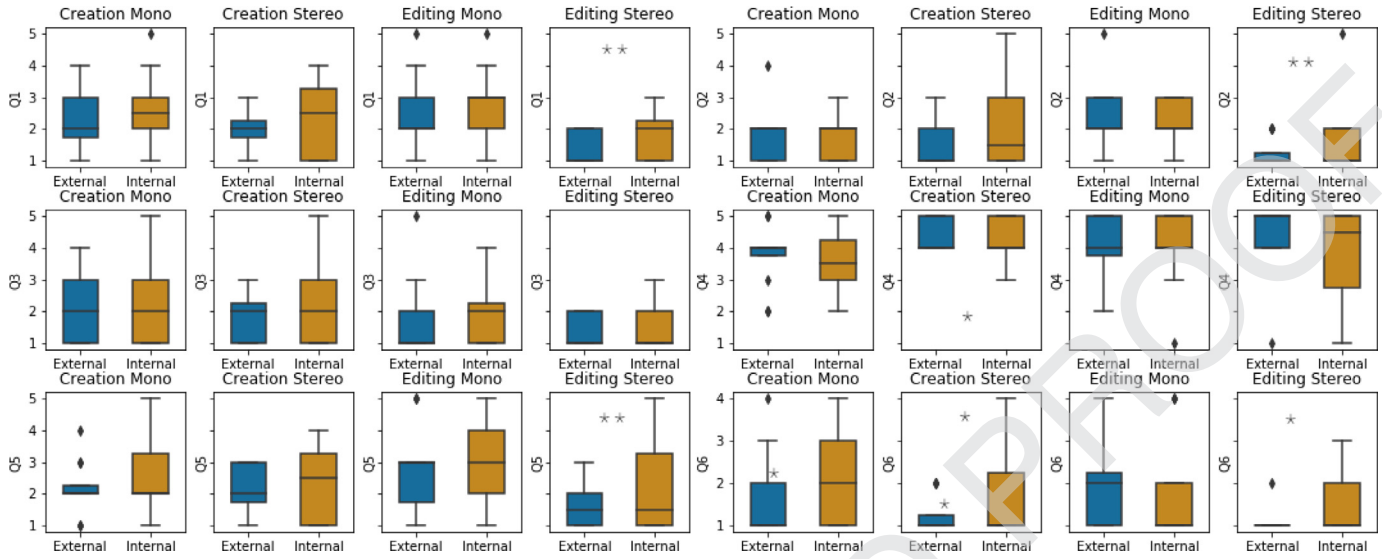


**Fig. 13. Qualitative evaluation.** Boxplots of answers in Likert scale for questions in Table 6 for two different editing metaphors (external and internal), two different setups (Mono and Stereo), and two different tasks (creating and editing). The bottom and top of each box are the first and third quartiles, the black line inside the box is the second quartile (the median), and the ends of the whiskers extending vertically from the boxes represent the lowest datum still within 1.5 IQR (inter-quartile range) of the lower quartile, and the highest datum still within 1.5 IQR of the upper quartile.

**Table 6**
**User evaluation:** 12 subjects were asked to compare two different editing metaphors (external and internal) on two different setups (Mono and Stereo) for two different tasks (creating and editing). Table shows the results of the answers of a 6-item questionnaire [?] on a Likert scale (1=low,5=high).

| Question | **Results** (Likert scale: 1=low 5=high) | | | | | | | |
|---|---|---|---|---|---|---|---|---|
| | Creation | | | | Editing | | | |
| | Stereo | | Mono | | Stereo | | Mono | |
| | External | Internal | External | Internal | External | Internal | External | Internal |
| **Q1**: How mentally demanding was it? | $2.0 \pm 0.7$ | $2.4 \pm 1.2$ | $2.2 \pm 0.9$ | $2.7 \pm 1.1$ | $1.4 \pm 0.5$ | $1.8 \pm 0.8$ | $2.5 \pm 1.1$ | $2.7 \pm 1.2$ |
| **Q2**: How physically demanding was it? | $1.4 \pm 0.7$ | $2.0 \pm 1.3$ | $1.8 \pm 0.9$ | $1.7 \pm 0.7$ | $1.3 \pm 0.5$ | $1.6 \pm 1.2$ | $2.3 \pm 1.1$ | $2.3 \pm 0.7$ |
| **Q3**: How hurried was the pace? | $1.9 \pm 0.8$ | $2.2 \pm 1.3$ | $2.1 \pm 1.2$ | $2.3 \pm 1.3$ | $1.3 \pm 0.5$ | $1.5 \pm 0.8$ | $1.8 \pm 1.2$ | $1.9 \pm 1.0$ |
| **Q4**: How successful were you? | $4.3 \pm 0.5$ | $4.2 \pm 0.7$ | $3.8 \pm 1.0$ | $3.7 \pm 1.0$ | $4.4 \pm 1.2$ | $3.8 \pm 1.5$ | $3.9 \pm 1.1$ | $4.0 \pm 1.1$ |
| **Q5**: How hard did you have to work ? | $2.1 \pm 0.8$ | $2.3 \pm 1.3$ | $2.2 \pm 0.8$ | $2.7 \pm 1.2$ | $1.6 \pm 0.7$ | $2.2 \pm 1.5$ | $2.8 \pm 1.4$ | $3.0 \pm 1.2$ |
| **Q6**: How stressed were you? | $1.3 \pm 0.5$ | $1.7 \pm 1.1$ | $1.7 \pm 1.0$ | $2.3 \pm 1.1$ | $1.1 \pm 0.3$ | $1.6 \pm 0.8$ | $1.9 \pm 1.0$ | $1.7 \pm 1.2$ |

designed the duration of tests in a way to do not let subjects perceive any problem of cybersickness (maximum 10 minutes for each task, and 5 minutes break between the tasks), results of the user study appear to be in contradiction with respect to the evaluation performed by expert users during the tracing of entire cells. It was a conscious decision during the design of the user study, even if we are aware that it would be important to evaluate the effects of cybersickness and to find ways to reduce it. We plan to carry out further user study investigations in future, with different task duration, in order to better evaluate the effects of cybersickness and physical efforts on our framework.

### 7.3. Case study: Analysis of branch-based intracellular organelles.

One of the significant benefits of having skeleton representations of brain cells is the possibility of computing accurate measurements of morphological features. As a preliminary test, neuroscientists performed analysis of mitochondria, which are intracellular structures within the neural cells Neuron1 and Neuron2 (see Table 7). Since scientists are particularly interested in measuring specific geometric features of organelles, like lengths and radii (maximum, minimum, and average), adequate skeleton representations are needed for performing accurate measures. To this end, our system uses the same functionality equipped in the VR path stabilizer. Users can point at a particular node from a branch of interest, and the system uses the skeleton information for providing the measure of the full length, along with the radius values at each skeletal node contained in that branch. The measured values are shown as text labels in the scene on top of each node and recorded for subsequent statistical analysis (see Fig. 14).

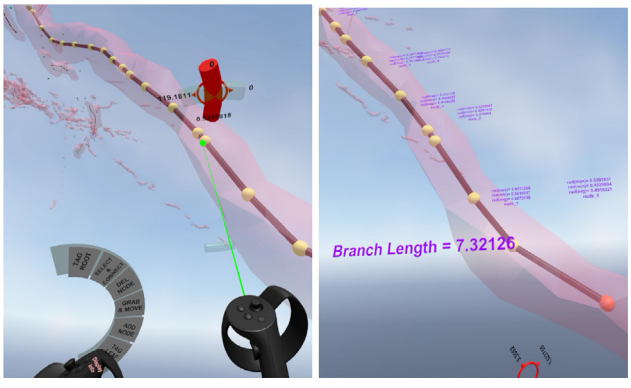


**Fig. 14. Branch-based measurements.** Our system performs calculations of measurements on intracellular structures. Left: User points the laser pointer at any node of a branch of interest to display node-relevant measurements. Right: Measurements of a mitochondrion branch are displayed.

UNCORRECTED PROOF

**Table 7**
The intracellular structures of Neuron1 and Neuron2 showing mitochondria morphology, side by side with their skeletons generated via the MCS algorithm.

| Cell Name | Morphology | MC Skeleton | Nodes\| Edges\| Branches |
|---|---|---|---|
| Mito Neuron1 | 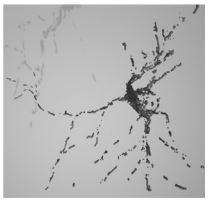 |  | 2246\| 1963\| 1396 |
| Mito Neuron2 | 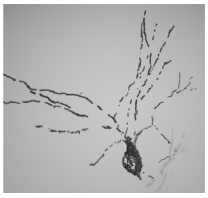 | | 1749\| 1656\| 811 |

## 8. Conclusion

We presented an immersive system for creating, proofreading and exploring medial axis representations from highly detailed brain cellular morphologies reconstructed from serial electron microscopy. The framework is designed for stereoscopic HMD display setups and extended to large-scale monocular displays in a way to alleviate unpleasant side-effects like cyber-sickness and fatigue, while still providing the ability to edit the skeleton in an immersive way. The system is currently used by neuroscientists for deriving accurate skeleton representations to be used for classification, measurements, and simulation purposes [8]. We presented the outcomes of a user study to evaluate and compare the strengths the proposed system.

Our subjective preliminary evaluation showed that domain scientists feel particularly comfortable in using the system for proofreading and editing previously computed skeletons while they still consider the process of creating medial axis representations from scratch to be comparable to automated or semi-automated 3D tools, in terms of time consumption, although they recognised how powerful the path stabilizer approach is to find the medial axis automatically, and the combination of external and internal tracing metaphors dramatically speed-up the creation process. Plans to improve the system include the implementation of online collaborative schemes, in order to distribute the creation process among multiple users, reduce the working time and effort, and at the same time increase the quality of the output representation; and integration of visual analytics tools for exploring feature distributions inside morphologies [59] and tools for performing visual analysis of topological data representations associated to medial axis representations [40]. Finally we customized the system for two different setups, considering direct metric interaction, and standard gaming indirect interfaces [54]. We did not yet investigate alternative interfaces that could speed-up the editing process and exploration, like touch-based systems to be attached to the display wall setup or gesture recognition systems to be attached to the stereoscopic HMD setup. We plan to explore this avenue, in order to understand which interface is more performing for these kind of neuroscience investigations.

## Declaration of Competing Interest

The authors declare that they have no known competing financial interests or personal relationships that could have appeared to influence the work reported in this paper.

## CRediT authorship contribution statement

**Daniya Boges:** Methodology, Formal analysis. **Marco Agus:** Methodology, Formal analysis, Supervision, Writing - original draft, Writing - review & editing. **Ronell Sicat:** Methodology, Supervision, Validation. **Pierre J. Magistretti:** Funding acquisition, Investigation, Formal analysis. **Markus Hadwiger:** Methodology, Supervision, Writing - review & editing. **Corrado Calì:** Project administration, Data curation, Methodology, Writing - review & editing.

## Acknowledgment

This work is supported by KAUST King Abdullah University of Science and Technology KAUST-EPFL Alliance for Integrative Modeling of Brain Energy Metabolism https://www.kaust.edu.sa/en under KAUST CRG6 Grant No. 2313. We thank all the participants of the user study from KAUST and from the Neuroscience Institute "Cavalieri Ottolenghi". We also thank the anonymous reviewers for useful comments and suggestions.

## Supplementary material

Supplementary material associated with this article can be found, in the online version, at doi:10.1016/j.cag.2020.05.024

## References

[1] Calì C, Agus M, Kare K, Boges D, Lehväslaiho H, Hadwiger M, et al. 3D cellular reconstruction of cortical glia and parenchymal morphometric analysis from serial block-face electron microscopy of juvenile rat. Prog Neurobiol 2019. In press
[2] Coggan JS, Keller D, Calì C, Lehväslaiho H, Markram H, Schürmann F, et al. Norepinephrine stimulates glycogenolysis in astrocytes to fuel neurons with lactate. PLoS Comput Biol 2018;14(8):e1006392.
[3] Markram H, Muller E, Ramaswamy S, Reimann M, Abdellah M, Sanchez C, et al. Reconstruction and simulation of neocortical microcircuitry. Cell 2015;163(2):456–92. doi:10.1016/j.cell.2015.09.029.
[4] Calì C, Baghabra J, Boges DJ, Holst GR, Kreshuk A, Hamprecht FA, et al. Three-dimensional immersive virtual reality for studying cellular compartments in 3d models from EM preparations of neural tissues: 3d virtual reality for neural tissue. J Comp Neurol 2016;524(1):23–38. doi:10.1002/cne.23852.
[5] Agus M, Boges D, Gagnon N, Magistretti PJ, Hadwiger M, Cali C. Glam: glycogen-derived lactate absorption map for visual analysis of dense and sparse surface reconstructions of rodent brain structures on desktop systems and virtual environments. Comput Graph 2018;74:85–98.
[6] Usher W, Klacansky P, Federer F, Bremer P-T, Knoll A, Yarch J, et al. A virtual reality visualization tool for neuron tracing. IEEE Trans Vis Comput Graph 2017;24(1):994–1003.
[7] Vezzoli E, Cali C, De Roo M, Ponzoni L, Sogne E, Gagnon N, et al. Ultrastructural evidence for a role of astrocytes and glycogen-derived lactate in learning-dependent synaptic stabilization. Cerebral Cortex 2019.

Please cite this article as: D. Boges, M. Agus and R. Sicat et al., Virtual reality framework for editing and exploring medial axis representations of nanometric scale neural structures, Computers & Graphics, https://doi.org/10.1016/j.cag.2020.05.024

UNCORRECTED PROOF

[8] Kanari L, Ramaswamy S, Shi Y, Morand S, Meystre J, Perin R, et al. Objective morphological classification of neocortical pyramidal cells. Cerebral Cortex 2019;29(4):1719–35. doi:10.1093/cercor/bhy339.
[9] Longair MH, Baker DA, Armstrong JD. Simple neurite tracer: open source software for reconstruction, visualization and analysis of neuronal processes. Bioinformatics 2011;27(17):2453–4.
[10] Schindelin J, Arganda-Carreras I, Frise E, Kaynig V, Longair M, Pietzsch T, et al. Fiji: an open-source platform for biological-image analysis. Nat Methods 2012;9(7):676.
[11] Schindelin J, Rueden CT, Hiner MC, Eliceiri KW. The imagej ecosystem: an open platform for biomedical image analysis. Mol Reprod Dev 2015;82(7–8):518–29.
[12] Tagliasacchi A, Delame T, Spagnuolo M, Amenta N, Telea A. 3d skeletons: A state-of-the-art report. In: Proceedings of the 37th Annual Conference of the European Association for Computer Graphics: State of the Art Reports. Goslar Germany, Germany: Eurographics Association; 2016. p. 573–97. doi:10.1111/cgf.12865.
[13] Boges D, Cal C, Magistretti PJ, Hadwiger M, Sicat R, Agus M. Immersive Environment for Creating, Proofreading, and Exploring Skeletons of Nanometric Scale Neural Structures. Smart Tools and Apps for Graphics - Eurographics Italian Chapter Conference. Agus M, Corsini M, Pintus R, editors. The Eurographics Association; 2019. ISBN 978-3-03868-100-7. doi:10.2312/stag.20191360.
[14] Mohammed H, Al-Awami A, Beyer J, Cali C, Magistretti PJ, Pfister H, et al. Abstractocyte: a visual tool for exploring nanoscale astroglial cell morphology.. PacificVis; 2017.
[15] Hadwiger M, Al-Awami A, Beyer J, Agus M, Pfister H. SparseLeap: Efcient Empty Space Skipping for Large-Scale Volume Rendering.; 2017.
[16] Keiriz J.J., Zhan L., Chukhman M., Ajilore O., Leow A.D., Forbes A.G.. Exploring the human connectome topology in group studies. arXiv preprint arXiv:1706102972017..
[17] Agus M, Gobbetti E, Iglesias Guitián JA, Marton F. Evaluating layout discrimination capabilities of continuous and discrete automultiscopic displays. In: Proc. Fourth International Symposium on 3D Data Processing, Visualization and Transmission; 2010.
[18] Hänel C, Pieperhoff P, Hentschel B, Amunts K, Kuhlen T. Interactive 3d visualization of structural changes in the brain of a person with corticobasal syndrome. Front Neuroinform 2014;8:42.
[19] Laha B, Sensharma K, Schiffbauer JD, Bowman DA. Effects of immersion on visual analysis of volume data. IEEE Trans Vis Comput Graph 2012;18(4):597–606.
[20] Agus M, Gobbetti E, Iglesias Guitián J, Marton F, Pintore G. Gpu accelerated direct volume rendering on an interactive light field display. Comput Graphics Forum 2008;27(3):231–40. Proc. Eurographics 2008
[21] Laha B, Bowman DA, Socha JJ. Effects of vr system fidelity on analyzing isosurface visualization of volume datasets. IEEE Trans Vis Comput Graph 2014;20(4):513–22.
[22] Forsberg A, Katzourin M, Wharton K, Slater M, et al. A comparative study of desktop, fishtank, and cave systems for the exploration of volume rendered confocal data sets. IEEE Trans Vis Comput Graph 2008;14(3):551–63.
[23] Alper B, Hollerer T, Kuchera-Morin J, Forbes A. Stereoscopic highlighting: 2d graph visualization on stereo displays. IEEE Trans Vis Comput Graph 2011;17(12):2325–33.
[24] Arsiwalla XD, Zucca R, Betella A, Martinez E, Dalmazzo D, Omedas P, et al. Network dynamics with brainx3: a large-scale simulation of the human brain network with real-time interaction. Front Neuroinform 2015;9:2.
[25] Xu R, Thomas MM, Leow A, Ajilore OA, Forbes AG. Tempocave: Visualizing dynamic connectome datasets to support cognitive behavioral therapy. In: 2019 IEEE Visualization Conference (VIS). IEEE; 2019. p. 186–90.
[26] Sobiecki A, Jalba A, Telea A. Comparison of curve and surface skeletonization methods for voxel shapes. Pattern Recogn Lett 2014;47:147–56. doi:10.1016/j.patrec.2014.01.012.
[27] Tagliasacchi A, Alhashim I, Olson M, Zhang H. Mean curvature skeletons. Comput Graph Forum 2012;31(5):1735–44. doi:10.1111/j.1467-8659.2012.03178.x.
[28] Yan Y, Sykes K, Chambers E, Letscher D, Ju T. Erosion thickness on medial axes of 3d shapes. ACM Trans Graph 2016;35(4):38:1–38:12. doi:10.1145/2897824.2925938.
[29] Livesu M, Attene M, Patané G, Spagnuolo M. Explicit cylindrical maps for general tubular shapes. Comput-Aided Des 2017;90:27–36.
[30] Li P, Wang B, Sun F, Guo X, Zhang C, Wang W. Q-Mat: computing medial axis transform by quadratic error minimization. ACM Trans Graph 2015;35(1):8:1–8:16. doi:10.1145/2753755.
[31] Yan Y, Letscher D, Ju T. Voxel cores: efficient, robust, and provably good approximation of 3d medial axes. ACM Trans Graph 2018;37(4):44:1–44:13. doi:10.1145/3197517.3201396.
[32] Sato M, Bitter I, Bender MA, Kaufman AE, Nakajima M. Teasar: Tree-structure extraction algorithm for accurate and robust skeletons. In: Proceedings of the 8th pacific conference on computer graphics and applications. Washington, DC, USA: IEEE Computer Society; 2000 http://dl.acm.org/citation.cfm?id=826029.826514. ISBN 0-7695-0868-5. 281–
[33] Westenberger P. Avizo-3d visualization framework. In: Geoinformatics conference; 2008. p. 1–11.
[34] Gillette TA, Ascoli GA. Topological characterization of neuronal arbor morphology via sequence representation: I-motif analysis. BMC Bioinformatics 2015;16(1):216.
[35] Gillette TA, Hosseini P, Ascoli GA. Topological characterization of neuronal arbor morphology via sequence representation: ii-global alignment. BMC Bioinform 2015;16(1):209.
[36] Li Y, Wang D, Ascoli GA, Mitra P, Wang Y. Metrics for comparing neuronal tree shapes based on persistent homology. PLoS One 2017;12(8):e0182184.
[37] Batabyal T, Acton ST. Neurosol: automated classification of neurons using the sorted laplacian of a graph. In: 2017 IEEE 14th international symposium on biomedical imaging (ISBI 2017). IEEE; 2017. p. 397–400.
[38] Batabyal T, Acton ST. Elastic path2path: automated morphological classification of neurons by elastic path matching. In: 2018 25th IEEE international conference on image processing (ICIP); 2018. p. 166–70. doi:10.1109/ICIP.2018.8451446.
[39] Riihimäki H., Chacholski W., Theorell J., Hillert J., Ramanujam R.. A topological data analysis based classification method for multiple measurements. arXiv preprint arXiv:1904029712019;.
[40] Kanari L, Dłotko P, Scolamiero M, Levi R, Shillcock J, Hess K, et al. A topological representation of branching neuronal morphologies. Neuroinformatics 2018;16(1):3–13. doi:10.1007/s12021-017-9341-1.
[41] Abdellah M, Hernando J, Eilemann S, Lapere S, Antille N, Markram H, et al. Neuromorphovis: a collaborative framework for analysis and visualization of neuronal morphology skeletons reconstructed from microscopy stacks. Bioinformatics 2018;34(13):i574–82.
[42] Titze B, Genoud C. Volume scanning electron microscopy for imaging biological ultrastructure. Biol Cell 2016;108(11):307–23. doi:10.1111/boc.201600024.
[43] Lichtman JW, Pfister H, Shavit N. The big data challenges of connectomics. Nat Neurosci 2014;17(11):1448–54.
[44] Coggan JS, Calì C, Keller D, Agus M, Boges D, Abdellah M, et al. A process for digitizing and simulating biologically realistic oligocellular networks demonstrated for the neuro-glio-vascular ensemble. Front Neurosci 2018;12. doi:10.3389/fnins.2018.00664.
[45] Sommer C, Straehle C, Köthe U, Hamprecht FA. Ilastik: Interactive learning and segmentation toolkit. In: 2011 IEEE international symposium on biomedical imaging: From nano to macro. IEEE; 2011. p. 230–3. doi:10.1109/ISBI.2011.5872394.
[46] Cardona A, Saalfeld S, Schindelin J, Arganda-Carreras I, Preibisch S, Longair M, et al. Trakem2 software for neural circuit reconstruction. PLoS One 2012;7(6):e38011. doi:10.1371/journal.pone.0038011.
[47] Agus M, Calì C, Al-Awami A, Gobbetti E, Magistretti P, Hadwiger M. Interactive volumetric visual analysis of glycogen-derived energy absorption in nanometric brain structures. Comput Graph Forum 2019;38(3):427–39.
[48] Murray JW. Building virtual reality with unity and steam VR. AK Peters/CRC Press; 2017.
[49] Desai P.R., Desai P.N., Ajmera K.D., Mehta K.. A review paper on oculus rift-a virtual reality headset. arXiv preprint arXiv:140811732014;.
[50] Dempsey P. The teardown: htc vive vr headset. Eng Technol 2016;11(7–8):80–1.
[51] Hess R. The essential blender: guide to 3D creation with the open source suite blender. No Starch Press; 2007.
[52] Cignoni P, Callieri M, Corsini M, Dellepiane M, Ganovelli F, Ranzuglia G. Meshlab: an open-source mesh processing tool.. In: Eurographics Italian chapter conference, 2008; 2008. p. 129–36.
[53] Maraj C, Hurter J, Ferrante S, Horde L, Carter J, Murphy S. Oculus rift versus htc vive: usability assessment from a teleportation task. In: International conference on human-computer interaction. Springer; 2019. p. 247–57.
[54] Mendes D, Caputo FM, Giachetti A, Ferreira A, Jorge J. A survey on 3d virtual object manipulation: from the desktop to immersive virtual environments. In: Computer graphics forum, 38. Wiley Online Library; 2019. p. 21–45.
[55] Calì C, Baghabra J, Boges DJ, Holst GR, Kreshuk A, Hamprecht FA, et al. 3D Immersive virtual reality for studying cellular compartments in 3D models from EM preparations of neural tissues. J Comp Neurol 2016;524(1):23–38.
[56] Jaeger S, Klein K, Joos L, Zagermann J, de Ridder M, Kim J, et al. Challenges for brain data analysis in vr environments. In: 2019 IEEE pacific visualization symposium (PacificVis). IEEE; 2019. p. 42–6.
[57] Hart SG. Nasa-task load index (nasa-tlx); 20 years later. In: Proceedings of the human factors and ergonomics society annual meeting, 50. Sage Publications Sage CA: Los Angeles, CA; 2006. p. 904–8.
[58] Taha AA, Hanbury A. An efficient algorithm for calculating the exact hausdorff distance. IEEE Trans Pattern Anal Mach Intell 2015;37(11):2153–63.
[59] Sicat R, Li J, Choi J, Cordeil M, Jeong W-K, Bach B, et al. Dxr: a toolkit for building immersive data visualizations. IEEE Trans Vis Comput Graph 2018;25(1):715–25.

UNCORRECTED PROOF

Please cite this article as: D. Boges, M. Agus and R. Sicat et al., Virtual reality framework for editing and exploring medial axis representations of nanometric scale neural structures, Computers & Graphics, https://doi.org/10.1016/j.cag.2020.05.024